

Recovery of Oil from Palm Oil Mill Effluent using Polypropylene Micro/nanofiber

Veroneka Semilin^a, Jidon Janaun^{a,d,*}, Chung Chin Hing^{a,e}, Dalila Touhami^b, Stephanie K. Haywood^b,
Chong Khim Phin^d, Abu Zahrim Yaser^{a,d} & Sharif H Zein^c,

^a*Faculty of Engineering, Universiti Malaysia Sabah, Jalan UMS, 88400, Kota Kinabalu, Sabah, Malaysia*

^b*School of Engineering, Faculty of Science and Engineering University of Hull, Cottingham Road, Hull,
HU6 7RX, United Kingdom*

^c*Department of Chemical Engineering, Faculty of Science and Engineering, University of
Cottingham Road, Hull, Hull, HU6 7RX, United Kingdom*

^d*Sustainable Palm Oil Research Unit (SPOR), Universiti Malaysia Sabah, Jalan UMS, 88400, Kota
Kinabalu, Sabah, Malaysia*

^e*Biosain Technologies Sdn. Bhd., Bloack 11, Lot 94, Ground Floor, Phase 11, Prima Square, Batu 4,
Jalan Utara, P. O. Box 77, 90701 Sandakan, Sabah, Malaysia.*

*Corresponding author: jidon@ums.edu.my

Abstract

1. Introduction

In palm oil mill industry, oil losses during the milling process are unavoidable. The main sources of oil losses are through wastewater clarification, sterilizer condensate and hydro-cyclone, which affect the oil extraction rate, % (OER) and the oil extraction efficiency, % (OEE) of the mills [1], [2]. In palm oil milling process, palm oil mill effluent (POME) is the largest waste generated where 2.5 tons of POME are produced from the average in every ton of oil extracted and typical raw POME contains about 1% or range in 4,000 mg/L of oil and grease [3]–[5]. The presence of residual oil in POME may cause serious environmental pollution due to elevation of biological oxygen demand (BOD) and chemical oxygen demand (COD) values, which could be detrimental to aquatic organisms and surrounding habitats if untreated [6]. High concentration of BOD and COD values means high presents of organic matter, thus high consumption of oxygen for the microorganisms to decompose the organic matter [7]. Therefore, against the oil layer could reduce the biological activity of conventional biological ponding system since the suspended

32 microbes are surrounded by oil layer. Hence, the presence of residual palm oil in the river ought
33 to be regarded as hazardous material in order to safeguard the environment. In light of this, palm
34 oil mills are typically required by the local authority to treat POME to meet stringent limits before
35 the POME can be discharged into the environment.

36 Effective and efficient treatment of POME still remain a challenge for the palm oil millers
37 because of the nature of the residual oil in the POME. The residual oil in POME can be classified
38 into four measured size, such as free oil ($>150\ \mu\text{m}$), dispersed oil mixture ($20\text{-}150\ \mu\text{m}$), emulsified
39 oil ($5\text{--}20\ \mu\text{m}$) and soluble oil mixture ($<5\ \mu\text{m}$) [8]. The free oil in POME could easily be removed
40 by the conventional techniques, such as skimming or gravitational separation as it is readily
41 floating to the surface [9]. However, the dispersed oil and other smaller oil in the water phase
42 causing the oil not readily separable using conventional techniques, hence derived into oil losses.

43 The oil losses mean losing profit annually. The production of palm oil keeps in increasing
44 globally due to the high demand in the food industry and consumer products. This causes an
45 increase in the amount of POME. Often times, the approach is to breakdown the pollutants to
46 achieve the allowable discharge limits set by the government regulations such as open ponding
47 treatment [1], biological wastewater treatment [10], membrane filtration [3], a series of treatment
48 process in aerobic and anaerobic digestion (i.e. sedimentation-coagulation-flocculation) [11], [12]
49 and physiochemical treatment [13]. Recently, more efforts are done to recover the residual oil in
50 the POME by using oil trap tank [14]. Recovering the residual oil gives double benefits which are
51 reducing the organic loads in the POME and also increasing the OER.

52 Adsorption using sorbent is likely the most feasible and effective technique in recovery of
53 residual oil in water [15]. The sorbent property such as hydrophobic and oleophilic, are the most
54 important factor in oil-water adsorption process. In general, adsorption in oil-water mixture
55 involved three steps; adhesion and diffusion of oil into the sorbent surface, adsorb the oil through

56 capillary action, and lastly coalescence of oil droplets through intermolecular forces on the sorbent
57 structures [16]. Several sorbents have been reported such as rubber powders [17]; kapok fibrous
58 [18]; chitosan , bentonite, activated carbon [19]; and fly-ash boiler [20]. These sorbents are stated
59 to be represent as an effective oil recovery because of high oil adsorption capacity and
60 environmental friendly. However, these techniques have not been commercialized most likely due
61 to the uneconomical and lack of practicality reasons such as reusability and separation after
62 adsorption [21], [22].

63 In marine and petroleum industry, adsorption using fibrous sorbent materials, both natural and
64 synthetic based have been well established. Several researches such as, adsorption capacity,
65 reusability, adsorption using several type of oil and separation after adsorption were reported [23]–
66 [26]. Despite the fact that PP based fibrous sorbent have been investigated as an ideal materials
67 for oil removal in marine oil-spill due to its low density, low water uptake and excellent physical
68 and chemical resistance [27], the availability of material and feasible fabrication using melting
69 process is one of its advantages. Recently, the number of plastic wastes that composed from
70 polymers increased since it were first introduced [28]. Amongst other, PP is the second highest
71 percentage of waste produced after low density polyethylene (LDPE) [28]. Therefore, the
72 availability of the material is easily to obtain, at the same time helps to reduce the number of plastic
73 waste produced.

74 In this paper, a novel work on using polypropylene micro/nanofiber (PP-MNF) to recover
75 residual oil from POME is reported. The oil recovery from PP-MNF that consists of adsorption

76 and extraction processes, reusability and regeneration of used PP-MNF, quality of the oil extracted
77 and the physiochemical study of the PP-MNF are well presented.

78 **2. Methods**

79 *2.1. Preparation of polypropylene micro/nanofiber*

80 In this work, PP-MNF was used as the oil adsorbent to recover residual oil from POME. The
81 PP-MNF was produced using melt blowing equipment (Zetta Co. Ltd., Japan) in the Faculty of
82 Engineering, Universiti Malaysia Sabah and assembled like bundle of loose cotton. The melt
83 blowing equipment consisted of four major components such as extruder, die assembly, web
84 formation and winding. The PP granular powder (PP, Sun-Allomer) was gravity fed from the
85 hopper to the extruder and heated at 300°C, to melt the PP. Then, the rotating screws carried the
86 melted PP, to the die assembly at 10 Hz and sprayed through spinneret (0.8 mm of diameter) to a
87 collector or web formation, at a distance of 2.4 m. Hot air, also called as winding was supplied at
88 a maximum flow rate (approximately 25 m³/min).

89 *2.2. Sample of POME*

90 The POME sample was collected from a local palm oil mill located in Kota Marudu, Sabah,
91 Malaysia. The collection was in the combined POME pit, which is the location before the
92 wastewater flows into the cooling pond. The POME sample collected was kept in 18 gallons
93 containers and stored at room temperature for further experiment.

94 *2.3. Determination of oil adsorption capacity*

95 The determination of oil sorption capacity of PP-MNF was conducted using refined palm oil
96 (Vesawit Cooking Oil). A 400 mL of oil was prepared into a 1000 mL beaker and 1 g of raw PP-
97 MNF was weighed (W_0). Then, the PP-MNF was immersed in the oil for 10 min to allow for

98 complete adsorption and soaking process. The PP-MNF was removed and suspended for 1 min to
99 remove the loosely attached oil on the fiber. Next, the PP-MNF with oil adsorbed was weighed
100 (W_1). The determination of oil adsorption capacity is expressed by gravimetric basis as in Eq. (1).

$$101 \text{ Oil adsorption capacity (g of oil/g of MNF) = } (W_1 - W_0)/W_0 \quad \text{Eq. (1)}$$

102 Then, the extraction of oil from the PP-MNF was done manually using pressing technique by both
103 hands with wearing glove. The oil was collected and weighed ($W_{oil, pressed}$). Afterward, the pressed
104 PP-MNF was weighed (W_2).

105 The extraction yield by the pressing technique is expressed by the weight of oil extracted from
106 pressing divided by the weight of oil adsorbed on PP-MNF as quoted in Eq. (2). Whilst, the specific
107 oil pressing capacity is expressed as the weight of oil extracted from pressing divided by the weight
108 of raw fiber which quoted in Eq. (3).

$$109 \text{ Pressing extraction yield (\%)} = ((W_{oil,pressed})/(W_1 - W_0)) \times 100\% \quad \text{Eq. (2)}$$

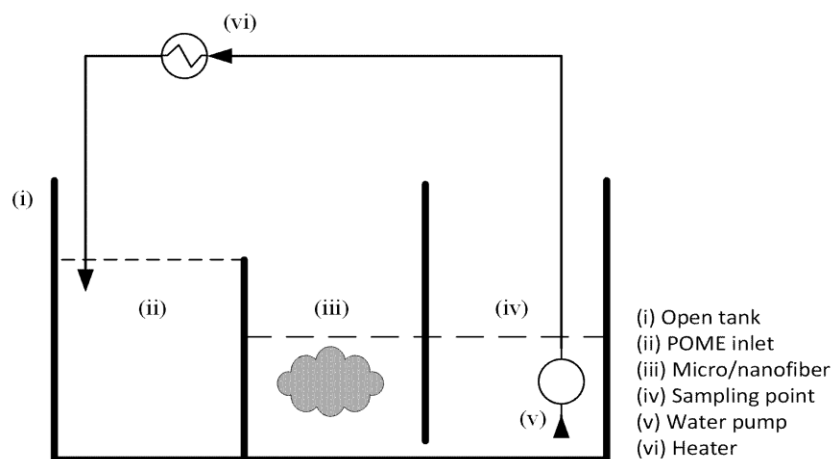
$$110 \text{ Specific Oil pressing capacity (g of Oil/g of MNF) = } (W_{oil,pressed})/W_0 \quad \text{Eq. (3)}$$

111 Despite the repeated pressing, there was oil retained in the PP-MNF assembly. The amount of
112 oil retained in the PP-MNF after repeated pressing was called as the oil retention capacity of the
113 fiber. The oil retention capacity of the PP-MNF is expressed as the weight of oil retained in PP-
114 MNF divided by the weight of raw PP-MNF as quoted in Eq. (4).

$$115 \text{ Oil retention capacity (g of oil/g of MNF) = } (W_2 - W_0)/W_0 \quad \text{Eq. (4)}$$

116 2.4. Recovery of residual oil from POME using PP-MNF

117 In order to evaluate the industrial applicability of the PP-MNF, it was used to recover residual
118 palm oil from the actual POME sample. In this works, the studies on oil recovery from POME
119 which consisted of adsorption and extraction process were performed using an experimental setup
120 shown in Figure 1. Figure 1 shows the schematic diagram of the experimental setup for oil
121 adsorption process from POME. The tank consisted of three compartments. The PP-MNF was
122 placed in the middle of the tank to ensure the maximum contact between POME and PP-MNF.
123 The tank was filled with 18 L of POME sample that was collected from a local palm oil mill and
124 was used as received without any pretreatment. A pump was used to recirculate the POME to
125 create flow in the tank as well as distributing the heat as desired. Heating was required in order to
126 achieve the desired temperature of the POME to imitate the actual temperature of POME in the
127 mill.



128
129 **Figure 1.** The schematic diagram of the experimental set up for oil adsorption process using PP-MNF. The
130 open tank (i) was divided into three compartments; POME inlet (ii), adsorption process using PP-MNF (iii)
131 and sampling point (iv). This system was supported by 600 L/h of water pump (v) to recirculate the POME
132 and heater (vi) that was set at 60°C.

133 2.4.1. Adsorption of residual oil from POME

134 To begin with, 1 g of raw PP-MNF (A_0) was placed in the middle of the tank and let it immersed
135 gravitationally in the POME and was run for 12 h [29]. Then, the PP-MNF was removed and
136 suspended for 1 min to drain out water and the loosely attached oil on the PP-MNF. The PP-MNF
137 with adsorbate was weighed (A_1). Three replication have been performed, to determine the
138 optimum adsorption capacity and oil recovery from POME using one g of PP-MNF. The total oil
139 content in the system ($A_{oil, system}$) was implied by determining the oil concentration in the POME
140 sample, where 250 mL sample was collected from sampling point for initial and final oil
141 concentration using the Standard Method of Oil and Grease Determination [30].

142 2.4.2. Extraction of oil from the PP-MNF

143 Subsequently, the extraction of oil from the PP-MNF was performed by hand pressing. The
144 pressing was done until no more droplets detached from the PP-MNF. The completely pressed PP-
145 MNF was weighed and labelled as A_2 . The extracted adsorbate was weighed ($A_{adsorbate, pressed}$),
146 subsequently dewatered in oven at 104-106 °C overnight. Then, the dewatered adsorbate was
147 mixed with 100 mL of n-hexane and filtered using vacuum filter to remove the solid particles. The
148 filtrate was then heated in a distillation unit to evaporate and to recover the solvent. The extracted
149 oil was weighed and labelled as $A_{oil, pressed}$.

150 In this technique, the pressing yield was calculated by dividing the weight of adsorbate that
151 pressed from the PP-MNF and the weight of adsorbate that adsorbed on the PP-MNF, which
152 quoted as Eq. (5).

153
$$POME \text{ pressing extraction yield (\%)} = ((A_{adsorbate, pressed}) / (A_1 - A_0)) \times 100\% \quad \text{Eq. (5)}$$

154 Whilst, the specific oil pressing capacity from POME was calculated by using Eq. (6).

155
$$\text{Specific Oil pressing capacity (g of Oil/g of MNF)} = (A_{oil,pressed})/A_0 \quad \text{Eq. (6)}$$

156 Then, the oil recovery efficiency was calculated as the weight of oil extracted divided by the total
157 oil content in the system, as expressed in Eq. (7)

158
$$\text{POME oil recovery efficiency (\%)} = ((A_{oil,pressed})/(A_{oil,system})) \times 100\% \quad \text{Eq. (7)}$$

159 The retention capacity was determined by calculating the weight of adsorbate that retained in the
160 PP-MNF ($A_2 - A_0$) divided by the weight of raw PP-MNF (A_0), which similar to Eq. (8).

161
$$\text{Oil retention capacity (g of oil/g of MNF)} = (A_2 - A_0)/A_0 \quad \text{Eq. (8)}$$

162 2.5. Reusability of PP-MNF

163 The reusability of the PP-MNF was evaluated by recycling the pressed PP-MNF. The
164 procedures in Section 2.4.1 and Section 2.4.2 were repeated by using another 1 g of PP-MNF,
165 which then recycled for 19 times in 18 L of fresh POME.

166 2.6. Extraction of oil from Pressed PP-MNF using chemical extraction

167 2.6.1. Solvent extraction

168 The solvent extraction was performed on the pressed PP-MNF (A_2) from Section 2.4.2. In the
169 solvent extraction technique, the PP-MNF was soaked in 100 ml n-hexane (99% purity) and gently
170 stirred for about 10 min to ensure complete contact between the solvent and the oil in the PP-MNF.
171 The washed PP-MNF was then suspended for 1 min to drain out excess n-hexane and removed

172 from the beaker, subsequently dried in an oven at 70 °C for 30 min. Then, the PP-MNF was
173 weighed (A_3). The solvent solution was filtered using vacuum pump to remove solid particles and
174 drained using separator funnel through 10 g of anhydrous sodium sulphate, to eliminate water
175 droplets. Then, it was distilled using evaporator to extract the oil and to recover the solvent. The
176 extracted oil was weighed ($A_{oil, solvent}$) and stored for oil analysis.

177 The extraction yield was determined by calculating the weight of oil extracted divided by the
178 initial weight of PP-MNF; as expressed in Eq. (9)

$$179 \text{ Solvent extraction yield (\%)} = ((A_2 - A_3)/A_2) \times 100\% \quad \text{Eq. (9)}$$

180 Eventually, the specific oil extraction capacity using solvent was calculated by dividing the weight
181 of extracted oil using solvent extraction with the weight of raw PP-MNF as shown in Eq. (10).

$$182 \text{ Solvent specific oil extraction capacity (g of oil/g of MNF)} = (A_{oil, solvent})/A_0 \quad \text{Eq. (10)}$$

183 2.6.2. Carbon dioxide supercritical extraction technique

184 The supercritical CO₂ extraction also performed on the pressed PP-MNF from Section 2.4.2
185 and carried out at the University of Hull laboratory facility. A 0.5 g of sample from pressed PP-
186 MNF (S_2) was extracted by using supercritical CO₂. Supercritical CO₂ technique was performed
187 in a Pyrex container placed inside a water-jacketed stainless steel cell (Parr®) rated to operate at
188 maximum of 300 bar (30 MPa). CO₂ (99.95%) was supplied to the high pressure cell from a
189 cylinder equipped with a dip tube. The pressures were adjusted (± 0.5 bar) by employing a JASCO
190 BP-2080-81 back pressure regulator and the flow rate was maintained at 2 mL/ min using JASCO
191 CO₂ delivery pump. The temperature was maintained at the desired values using a thermostatic

192 water circulator (± 0.01 °C). The extraction experiments were conducted in a batch manner. After
193 the required extraction time, the high pressure cell was slowly depressurized and the extract was
194 dissolved in heptane (99%) for analysis. The extract fiber was weighed (S_3) and the extracted oil
195 ($S_{oil, supercritical}$) was calculated by subtracting the initial and final extracted fiber ($S_2 - S_3$).

196 The extraction yield and its capacity were determined using equations as in Eq. (9) and Eq.
197 (10), respectively.

198 2.7. Characterization of PP-MNF and oil extracted

199 2.7.1. Physiochemical properties of PP-MNF

200 The physical and chemical changes of the PP-MNF were analyzed over six samples (before,
201 during and after use); such as raw PP-MNF, saturated PP-MNF, pressed PP-MNF, washed PP-
202 MNF, S-CO₂ PP-MNF and reused PP-MNF. The morphology of the PP-MNF were observed by
203 using a scanning electron microscopy (SEM). All but saturated PP-MNF samples were coated with
204 a layer of gold sputtering coater for 100 s to minimize the charging effect, whilst saturated PP-
205 MNF was undergone in cold stage imaging, where the sample was frozen to stabilize water. The
206 average of diameter on the PP-MNF was also measured using image processing software on the
207 SEM images.

208 The chemical composition of polypropylene based PP-MNF were analyzed using energy
209 dispersive X-ray (EDX) spectrometer connected to the SEM. The changes of bonding
210 configuration by determining the functional group were characterized by using Fourier transform
211 infrared (FTIR, Cary 360).

212

213 2.7.2. *Components distribution of oil extracted*

214 The oil recovered from the PP-MNF was analyzed on a gas chromatograph (HP6890)
215 connected to a mass spectrometer (HP5973), to determine the components distribution in the
216 extracted oil. The column used for the analysis was Stabilwax® (30 m x 0.32 mm ID x 0.25 µm).
217 The injection temperature was maintained at 250 °C. The oven temperature was maintained 210
218 °C for 5 min then raised to 230 °C at a gradient of 20 °C/min.

219 **3. Results and discussion**

220 3.1. *Oil adsorption capacity of the PP-MNF*

221 The study of oil recovery from POME using PP-MNF was initiated by determining the actual
222 oil adsorption capacity using clean and refined oil. The determination of PP-MNF sorption
223 capacity using refined palm oil is shown in Table 1. The results showed the adsorption capacity of
224 the PP-MNF was ranged from 26.96 to 30.17 g of oil/g of PP-MNF. As in average, the PP-MNF
225 could adsorbed about 28.65 g of oil/g of PP-MNF. This result was higher compared to Rengasamy
226 [31] and Ying [26], where the adsorption capacity of polypropylene fibers using high density oil
227 were 18.8 g of oil/g of fiber and 10 g of oil/g of fiber, respectively. These results can be justified
228 by the active surface area and its diameter [16]. The oil sorption capacity is increase, when the
229 active surface area also increase. The surface area is depends on the sorbent diameter. The diameter
230 of the PP-MNF in this work, was determined in between of micro and nano scale (0.1 - 1 µm),
231 which smaller than other polypropylene fibers; such as 19 µm [31] and 10 -15 µm [26]. Hence, the
232 PP-MNF has more active surface.

233 Furthermore, the adsorption process was observed to occur very fast and completely saturated
234 after 8 to 10 s. This phenomenon was likely associated with oleophilic properties of the PP-MNF.
235 The oleophilic properties, also known as oil-lover present because of non-polar surface area

236 between PP-MNF and oil. Theoretically, polypropylene has a long chain of hydrocarbon group,
 237 consist of CH and CH₂ group with a CH₃ pendant group, which makes the PP-MNF a very non-
 238 polar solid molecule [32]. Whilst, the refined palm oil is also a non-polar molecule, as it consists
 239 of a long chain of hydrocarbon group which is triglycerides [33]. According to Wade [32], when
 240 non-polar molecules are mixed with non-polar molecules, a weak intermolecular force is present
 241 between them and this intermolecular force is called London dispersion force. The London
 242 dispersion force is one of the van der Waals forces often present in a non-polar solute dissolves in
 243 non-polar solvent [34]. It is correlated to the attraction between two non-polar molecules and two
 244 temporary dipole are induced together. Hence, it is called induced dipole-induced dipole
 245 interactions [34]. Therefore, the adsorption of oil on the PP-MNF occurred due to the non-polar
 246 molecules attracted to each other by these weak intermolecular forces [32].

247 **Table 1.** Characteristic of refined palm oil sorption on the PP-MNF

Replication	Adsorption capacity (g of oil/ g of PP-MNF)	Extraction yield by pressing (%)	Specific Oil pressing capacity (g of oil/ g of PP-MNF)	Oil retention capacity (g of oil/ g of PP-MNF)
1	26.96	95.23	25.67	2.59
2	28.81	79.89	23.02	2.26
3	30.17	81.44	24.57	2.32
Average	28.65	85.52	24.42	2.39
SD	1.61	8.44	1.33	0.18

248

249 Despite the recovery of oil from the PP-MNF, the pressing technique showed that up to 95.23%
 250 of oil could be desorbed from the PP-MNF (Table 1). However, variation in the oil desorption
 251 yield occurred and showed average of 85.52% yield by pressing technique. The standard deviation
 252 was relatively high implying low reproducibility of the pressing technique. This could be due to
 253 the random error associated with low weight of PP-MNF used. Oil could stick on fingers during
 254 pressing and this oil loss could contribute significantly on the standard deviation because of the

255 little amount of PP-MNF used. Mechanized pressing that could deliver constant force and larger
256 amount of PP-MNF are expected to produce more reproducible data. The specific oil pressing
257 capacity showed average of 24.42 g of oil/g of PP-MNF, which indicated that approximately up to
258 20% of oil still remained in the PP-MNF (Table 1). Wade [32] further explained that the London
259 dispersion force requires only small energy to break the forces. This is because the temporary
260 dipoles are not always perfectly symmetrical, hence the induction to another non-polar will be
261 occasionally attracted. However, the attraction could be fairly strong when the size of molecules
262 increase [34]. This is because there are more opportunities for the induced dipole distortion. Hence,
263 there was oil retained in the PP-MNF after pressing.

264 The oil retention capacity of the PP-MNF after repeated pressing showed an average of 2.39 g
265 of oil/g of PP-MNF (Table 1). This result defined the minimum amount of oil retained in the PP-
266 MNF, hence the optimum pressing performed in desorption process. However, the oil retention
267 capacity is expected to be lower if the pressing was done at higher temperature as it was opposed
268 to the ambient temperature because high temperature could decrease the viscosity of the oil and
269 lower the molecules attractions [35]. According to Davarcioglu [34], the London dispersion force
270 could be affected by the fluid viscosity. High viscosity causes them to resist flow more strongly
271 because the attraction between molecules are strong. In fact, the viscosity is expected to be
272 temperature dependent. Hence, the extraction was intended for ambient condition. Moreover, the
273 oil retention capacity is a critical factor to be determined as excessive force could damage the fiber.

274 3.2. Recovery of oil from POME using PP-MNF

275 The actual application of the PP-MNF in industry is critical to be determined. For instance,
276 testing the capability of the PP-MNF to recover residual oil from POME is important because
277 POME contains not just oil but other materials such as water, organics, metals, and also suspended

278 solids [6]. In this study, the recovery of oil from POME consisted of oil adsorption and extraction
 279 studies. The adsorption process was done using the experimental setup as shown in Figure 1, whilst
 280 extraction was performed physically, by hand pressing. The initial oil content in the setup was
 281 determined by measuring the oil concentration of POME and obtained 34.42 to 44.45 g oil in 18
 282 L of POME (approximately 1900 - 2500 mg/L of initial concentration).

283 **Table 2.** Residual oil recovery from POME using pressing technique

Replication	Weight of oil in the system (g), $W_{oil, system}$	Adsorption capacity (g of adsorbate ^a / g of PP-MNF)	Extraction yield by pressing (%)	Specific Oil pressing capacity (g of oil/ g of PP-MNF)	Oil recovery efficiency of pressing (%)	Adsorbate retention capacity (g of adsorbate ^a / g of PP-MNF)
1	43.21	51.10	97.93	15.90	37.54	5.83
2	44.45	45.25	86.03	10.70	28.42	5.39
3	34.42	43.52	84.92	6.17	20.98	5.85
Average	40.69	46.62	89.62	10.93	28.98	5.69
SD	5.47	3.97	7.21	4.87	8.30	0.26

^a Adsorbate is a mixture of oil, suspended solid and water

284 3.2.1. Adsorption of oil from POME

285 During the adsorption process, the raw PP-MNF was initially observed floated on the POME
 286 surface. The floatation of the PP-MNF was due to the present of hydrocarbon chain from
 287 polypropylene, hence make it non-polar and hydrophobic (repel water) [16]. However, the raw
 288 PP-MNF was slowly sunk in the POME because of the oil adsorbed into the PP-MNF assembly.
 289 After 12 h, the PP-MNF was fully soaked and the color was changed into blackish yellow from
 290 white fiber. According to Alrawi [36], natural sediments mainly consist of solid particles and
 291 debris fibers from mesocarps that completely covered by the residual oil which believed due to the
 292 van der Waals interaction forces between them. This is why the PP-MNF became black due to the
 293 oily sediments adsorbed in the PP-MNF surface assembly, subsequently increased the capacity of

294 PP-MNF in POME than using refined palm oil. The result showed an average of 46.62 g of oil/g
295 of PP-MNF, for the adsorption capacity using POME (Table 2).

296 3.2.2. *Extraction of oil from POME by physical separation*

297 The oil adsorbed on the PP-MNF was extracted physically by hands pressing technique. The
298 pressing process obtained an oil that contained suspended solid (solid particles) and water.
299 Therefore, dewatering and oil filtration were carried out to remove water and filter the solid
300 particles in the oil by drying overnight in oven and diluting it with solvent and filtered using
301 vacuum filter, respectively.

302 Table 2 shows the pressing extraction yield and specific oil pressing capacity from the PP-
303 MNF. The results showed the yield by pressing extraction were ranging between 84.92 to 97.93%.
304 This result indicates that the pressing technique could be the potential desorption technique, as it
305 can desorbed more than 80% from its adsorption capacity. However, the specific oil pressing
306 capacity shows only 10.93 g of oil/g of PP-MNF was desorbed from the PP-MNF, while the rest
307 was solid particles, water and the oil that retained in the PP-MNF (Figure 2). Compared to the
308 refined palm oil adsorption capacity, this result showed a lot lower. This was suggested to the
309 difference between POME and refined palm oil behaviors. Rajakovic and co-workers [37] reported
310 that sorption in real oily wastewater have a very complex interactions between oil, surfactants and
311 wool fibers. Like POME, this oily wastewater from palm oil industry also have a complex mixture
312 due to the presence of water, residual oil and natural sediments [36]. Hence, that is why the
313 adsorption in POME contained of water and solid particles (Figure 2), subsequently lower the oil
314 adsorption capacity.

315 The low oil adsorption capacity could be explained by the effect of initial oil concentration
316 [16]. Low oil concentration need times to form an attraction between oil and the fiber surface.

317 Whilst, high oil concentration helps the PP-MNF occupies with oil and reach its saturation capacity
318 faster. The initial oil concentration in this work was ranged between 1900 – 2500 mg/L, which
319 provides an average of 40.69 g of oil in the whole system (Table 2). The PP-MNF should be able
320 to adsorb the oil, however due to emulsified oil dispersed in POME which mainly water, hence
321 reduced the probability of oil contact on the PP-MNF. This could be correlated to the attraction or
322 repulsion interactions between polar and non-polar molecules exist around the PP-MNF [34], thus
323 lower the oil adsorption capacity in 12 h contact time. Wahi and co-workers [16] explained that
324 increasing the contact time could increase the oil adsorption capacity, as well as oil removal from
325 the POME. Therefore, the oil adsorption capacity is expected to be increase as the contact time is
326 increased.

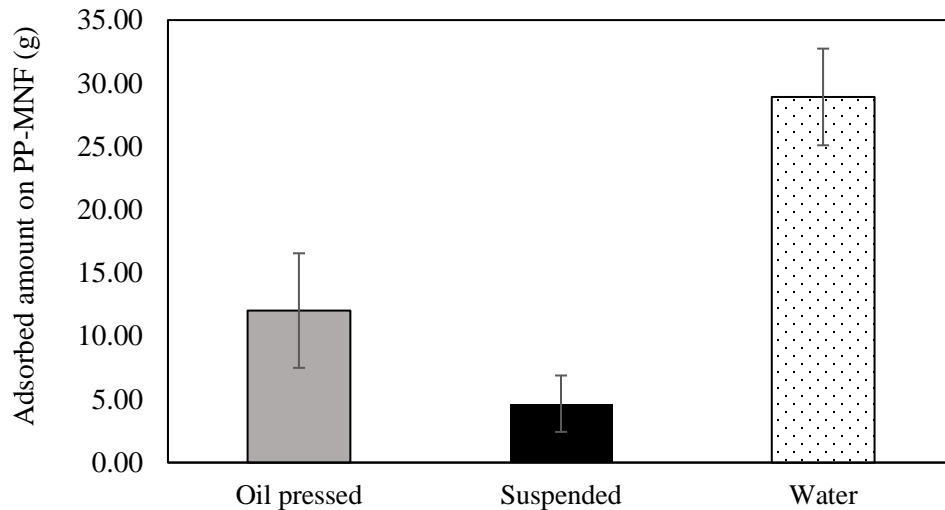
327 In addition, Table 2 shows the results of adsorbate retention capacity. In this work, adsorbate
328 defined as a mixture of residual oil, water and natural sediments that adsorbed on the PP-MNF
329 during the adsorption process. Thus, the adsorbate retention capacity is defined as the amount of
330 adsorbate retained in the PP-MNF. This also could defined as the maximum compression of the
331 PP-MNF with present of adsorbate, which important to be study because the fiber could be
332 damaged if excessive pressure was applied. The results showed average of 5.69 g of adsorbate/g
333 of PP-MNF that remained on the PP-MNF. This value higher than preliminary result, due to the
334 mixture of oil, water and suspended solid. However, the oil retained on the fiber could be desorbed
335 via chemical extraction due to its polarity effect [32].

336 3.2.3. *Characterization of Adsorbate Adsorbed on PP-MNF*

337 Adsorbate defined as a mixture of water, suspended solid and oil. Figure 2 shows the amount
338 of adsorbate that get adsorbed on the PP-MNF during the adsorption process. The histogram shows
339 that water adsorbed was higher than oil, followed by suspended solid. The results obtained is

340 suggest affected by the web assembly of the PP-MNF, which packed in loosely form (cotton-like)
341 fiber. The loose fiber assembly or fibers packing structure was noted has pore space between the
342 fibers, which measured around 10 – 50 μm (Figure 3a), thus attributes the large content of air gap.
343 The air gap in the fibers assembly provides a superhydrophobic surface [38], hence increase the
344 permeability of oil to the fibers wall through capillary when exposed with bulk of oil (refined palm
345 oil) [34]. However, when exposed with water bulk, the water would interact with air inside the
346 fibers (liquid-air interface), leading to water uptake [38]. Lim and Huang [34] suggested that the
347 interaction of water and air interface might begin when the external pressure (hydraulic pressure)
348 overcame the capillary entry pressure. The capillary entry pressure or also known as breakthrough
349 pressure is corresponds to the gravity, degree of saturation, pore size, pore shape and interfacial
350 forces [39]. Therefore, the PP-MNF assembly in this work might have overcame the capillary entry
351 pressure through the interfacial force (liquid-air interface), pore size and shape (cotton-like
352 assembly and air gap between the PP-MNF) and the adsorption under gravity process, which

353 results the penetrating of water in passing through the PP-MNF assembly (Figure 3a and Figure
354 3b).

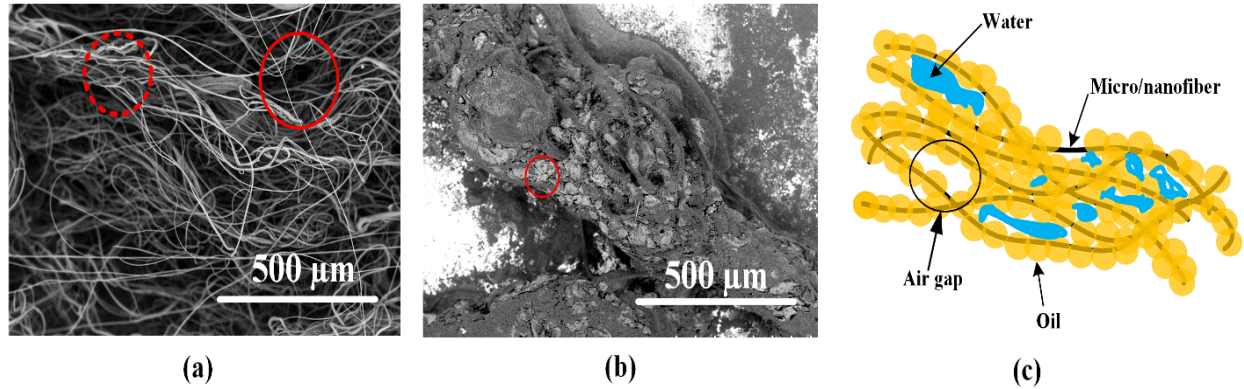


355

356 **Figure 2.** Amount of adsorbate adsorbed on the PP-MNF during adsorption process; oil pressed (grey bar),
357 solid particles (black bar) and water (dotted bar)

358 Despite the interaction of water and air gap between PP-MNF occurred during the adsorption
359 process, the interaction of PP-MNF and residual oil (adsorption process) also occurred based on
360 polarity effect and London dispersion force [34]. Hence, the phenomenon of water uptake during
361 the adsorption could explained by the water trapped between oil phases that adsorbed on the PP-
362 MNF assembly (Figure 3c). The water molecules would became unstable when interact with air in
363 the PP-MNF. This was likely due to repulsion forces present between water-oil and water-PP-
364 MNF (electronegativity effect) [40], [41] and break into droplets, then leads into water-oil
365 emulsion [9]. Figure 3c illustrates the water droplets in bulky oil phenomenon. The water droplets

366 dispersed in oil phase and trapped in the air gap between the PP-MNF, during the adsorption
367 process (Figure 3b).



369 **Figure 3.** SEM images of (a) Air gap in the PP-MNF assembly small (dotted red circle) and large (red
370 circle); (b) Dispersed water trapped between oil adsorbed on the PP-MNF (red circle); (c) Graphical
371 illustration of PP-MNF assembly during adsorption process.

372 Beside than water uptake, suspended solid also contributes in the adsorbate adsorption. The
373 suspended solid is mainly content of solid particles and silts (oily debris fiber) which also known
374 as natural sediments [36]. These natural sediments were investigated ranging from 38 to 1000 μm
375 and even less than 38 μm size of particles which found under the light microscopy [36]. These
376 solid particles were generated due the harsh pressing, stripping and digestion of fruit bunches and
377 the mesocarps [42], then mixed with the wastewater. Thus, the residual oil was attached or
378 adsorbed to the surface of the fibrous solid residues which believed due to non-polar surface and
379 capillary adsorption effect. Hence, these natural sediments were found on the PP-MNF during the
380 adsorption process because of the adhesion between oily sediments and the oleophilic surface on
381 the PP-MNF, as well as the pore space between the PP-MNFs (Figure 7k and Figure 7g).

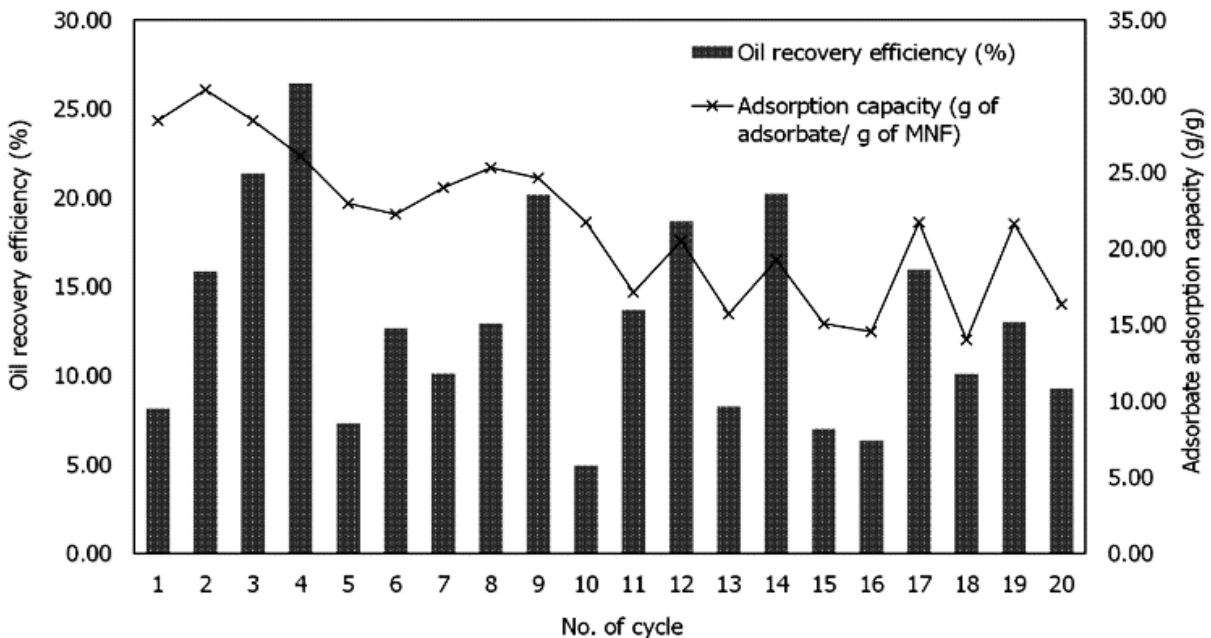
382 3.3. Reusability of used PP-MNF

383 The reusability of polypropylene PP-MNF had been studied over 20 batch of recycles. A 1 g
384 of clean and white PP-MNF was used at the first cycle and was further reused for 19 cycles of oil

385 adsorption and pressing technique for oil recovery, using fresh POME for every new cycle. The
 386 oil concentration of fresh POME was ranged between 3000 to 6000 mg/L (approximately 50.74 –
 387 112.94 g of oil in 18 L of POME volume).

388 Figure 4 shows the oil recovery efficiency and adsorption capacity of used PP-MNF over 20
 389 batch of recycling. The histogram results show a pattern of the oil recovery efficiency. An
 390 increased of oil recovery efficiency gradually from the first to the fourth reuse but suddenly
 391 dropped on the fifth reuse. This observation was consistent throughout the 20 cycles. This trend
 392 could be explained by the oil adsorption property of the PP-MNF. The interaction between the oil
 393 and PP-MNF occurs because of the hydrophobic property of the oil [43]. A sudden drop of the oil
 394 recovery efficiency after reaching the maximum capacity is most likely associated with the
 395 inability of the oil layer on the PP-MNF surface to attract oil from the bulk.

396



397

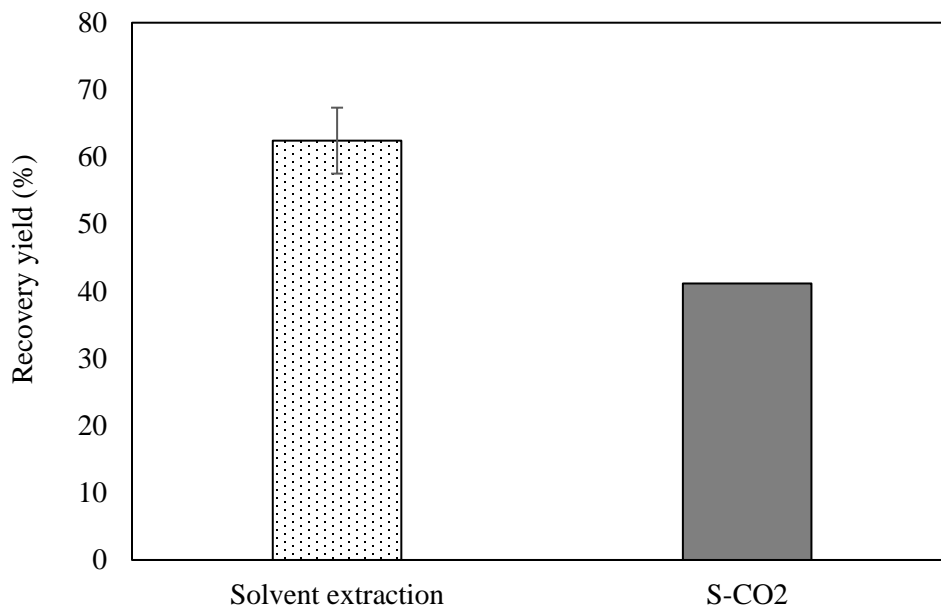
398 **Figure 4.** Efficiency of oil recovery and adsorption capacity from 1 g reused PP-MNF over 20 batch
 399 recycles using pressing technique

400 The capacity of PP-MNF in adsorption process can be seen decreases in Figure 4. At the
401 beginning of adsorption, the PP-MNF can adsorb more than 20 g of adsorbate/ g of PP-MNF. As
402 the PP-MNF was reused up to 20 cycles, the adsorbed capacity dropped gradually to 10 g of
403 adsorbate/ g of PP-MNF. This is likely due to the fouling effect on the PP-MNF [15], which was
404 caused by the natural sediments uptake [36] and non-extractable adsorbate using hand pressing
405 method. Nevertheless, the PP-MNF was still able to recover approximately 10 % of oil and
406 expected to recover another 10 % of oil, if re-used for more 5 to 10 cycles. In summary, these
407 results showed that polypropylene PP-MNF had a good reusability.

408 *3.4. Oil extraction by solvent extraction and supercritical-CO₂ techniques from pressed PP-MNF*

409 In this section, the non-extractable adsorbate on the pressed PP-MNF from Section 2.4.2 was
410 further extract using chemical extraction. Two techniques were performed to determine the
411 quantity of oil that retained on the PP-MNF; such as solvent washing [44] and supercritical-CO₂
412 [45]. Generally, these techniques called as solid-liquid extraction, where solvent is needed to
413 diffuse and desorb oil from the sorbent or samples [46]. In chemistry point of view, the non-polar
414 molecules of solvent will attract the non-polar molecules of residual oil through van der Waals
415 interaction and will repel the polar molecules like water [32]. Hence, two layer of solution were

416 observed. In addition, these works indirectly studied the regeneration of the PP-MNF [47]. Figure
417 5 shows the extraction yield from solvent washing and supercritical-CO₂.



418
419 **Figure 5.** Extracted oil from solvent extraction (dotted bar) and supercritical-CO₂ (grey) from pressed PP-
420 MNF

421 3.4.1. Extraction oil from PP-MNF using solvent washing

422 In solvent washing, n-hexane (99% purity) was used to wash the pressed PP-MNF. The pressed
423 PP-MNF consist adsorbate, such as oil and suspended solid. Water does present in the solvent
424 solution after washed, however the amount was negligible. Hence, anhydrous sodium sulphate was
425 used to adsorb the emulsion water in the solvent solution [11].

426 Most of researches reported that extraction using n-hexane gives highest oil yield [46], [48],
427 [49]. This solvent was used due to its non-polar molecules, where it consist of hydrocarbon group
428 that able to attract the same molecules in the residual oil. Like the general rule stated by Wade

429 [32], “like dissolves like” where non-polar substances will dissolve in non-polar solvents. Thus,
430 a single batch of solvent washing using n-hexane was done from the pressed PP-MNF.

431 Figure 5 shows that 62.44% of extraction yield obtained from the solvent extraction technique..
432 This could be due to the intermolecular forces between solvent, residual oil and the PP-MNF.
433 These three components were non-polar molecules [6], [16], [36], thus the potential of induced
434 dipole-induced dipole attraction was high and strong [34]. But, the interactions would depend on
435 its physical properties [50]. Solid molecules have strong intermolecular forces to keep neighbor
436 molecules locked besides them because the kinetic energy of solid molecules are lower than
437 liquids. The PP-MNF was a mass of solid non-polar molecules, hence it has stronger forces than
438 solvent and residual oil. The solvent and the residual oil were present in liquid form, thus the
439 kinetic energy of non-polar molecules were free to move past or slide over one another to form an
440 intermolecular forces [50]. Therefore, the oil retained in the PP-MNF was able to extract out due
441 to polarity effect.

442

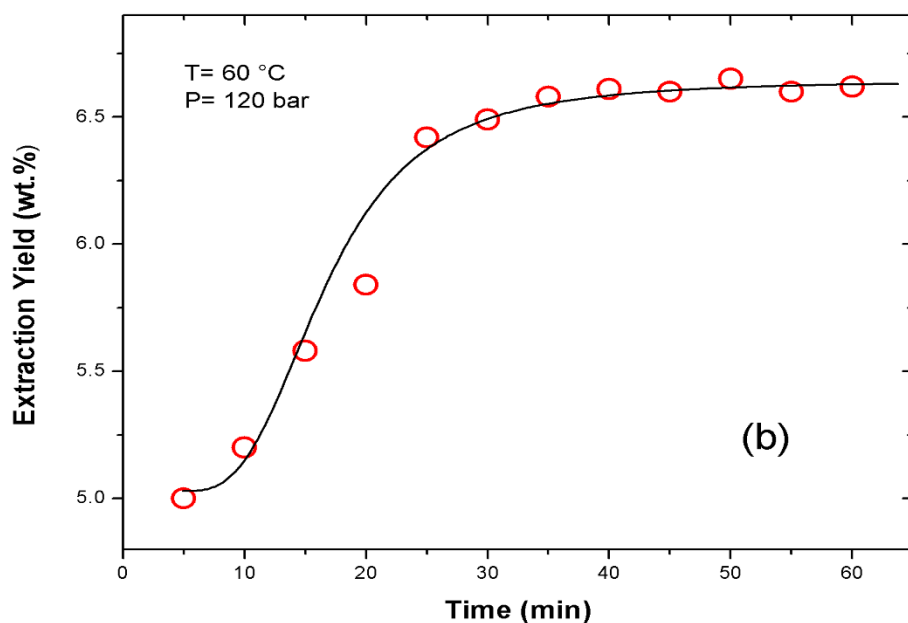
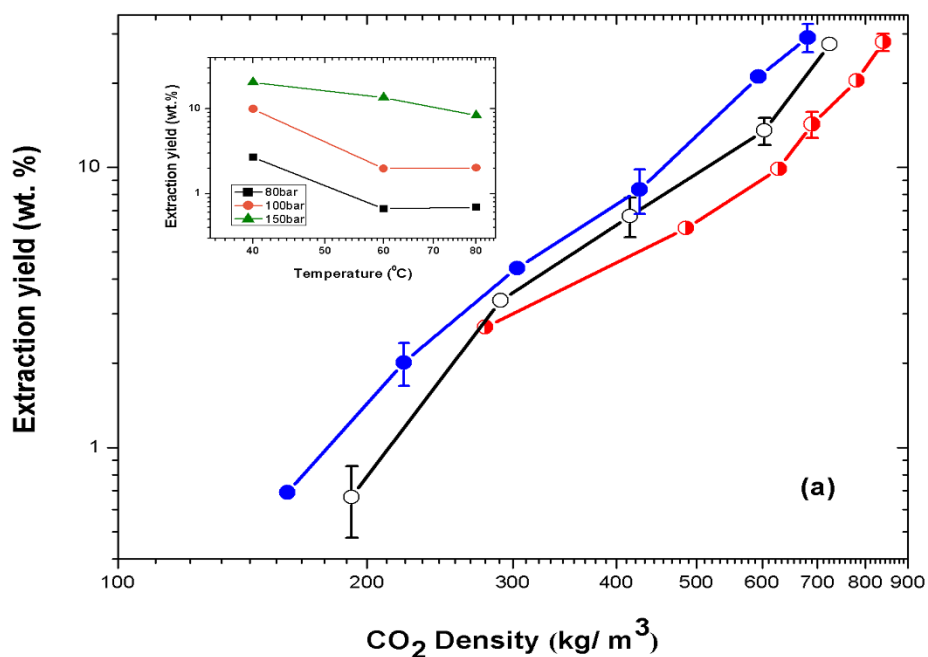
443 3.4.2. *Extraction oil from PP-MNF using supercritical-CO₂*

444 The effect of the CO₂ density on the extraction yield was studied at various temperatures (40
445 °C, 60 °C and 80 °C) and pressure range (80 to 200 bar). Temperature is a critical parameter which
446 affects the solubility and extraction capacity of the fluid [51]. Hence, temperature effect was
447 studied and the optimum condition was determined.

448 Figure 6 shows the yield of extraction using supercritical-CO₂ at various temperatures and
449 pressure range. Figure 6a inset shows the highest extraction yield is at its maximum (20 wt. %) for
450 40 °C at a particular pressure. The yield then decreases at least 4-folds with higher temperature up
451 to 100 bar (Figure 6a inset). Whereas, above 100 bar, the yield decreases only twice. This can be
452 explained by CO₂ density being highly affected by the temperature near the critical state. An

453 increase in temperature usually leads to a large decrease in fluid density which reduces oil
454 solubility in CO₂ hence the extraction yield [52]. This is clearly seen for the extractions carried out
455 at 60 °C and 80 °C (Figure 6a). At temperature above 60 °C, the pressure can be increased to at
456 least 120 bar to reach the density necessary for ca. 10 wt. % extraction yield.

457



458

459 **Figure 6.** Extraction yield dependence on CO₂ density at (a) 40 °C (half closed symbols) 60 °C (open
 460 symbols) 80 °C (closed symbols) at 80, 100, 120, 150 and 200 bar. Error bars indicate data scatter over
 461 three experiment at a particular CO₂ density. Inset- Extraction yield dependence on temperature at 80, 100
 462 and 150 bar. (b) Extraction yield dependence on time at 60 °C and 120 bar.

463 It is well accepted that high temperature increases the vapor pressure of the extractable
 464 compounds which enhances the extraction efficiency and accelerates mass transfer hence enhances

465 the yield [51]. However, in the current work the temperature was found to affect the yield only
466 when the pressure is increased beyond 100 bar where the CO₂ density is high enough for extraction.
467 This is not surprising since the solubility of oil is below very low (0.01 g oil per g of CO₂) at 40 °C
468 and pressure <100 bar [53], [54]. Figure 5b shows the extraction yield dependence on time at 60
469 °C and 120 bar. The extraction yield increases 1.3 folds over the first 25 min. The optimum
470 extraction time at which experiments were conducted was 35 min.

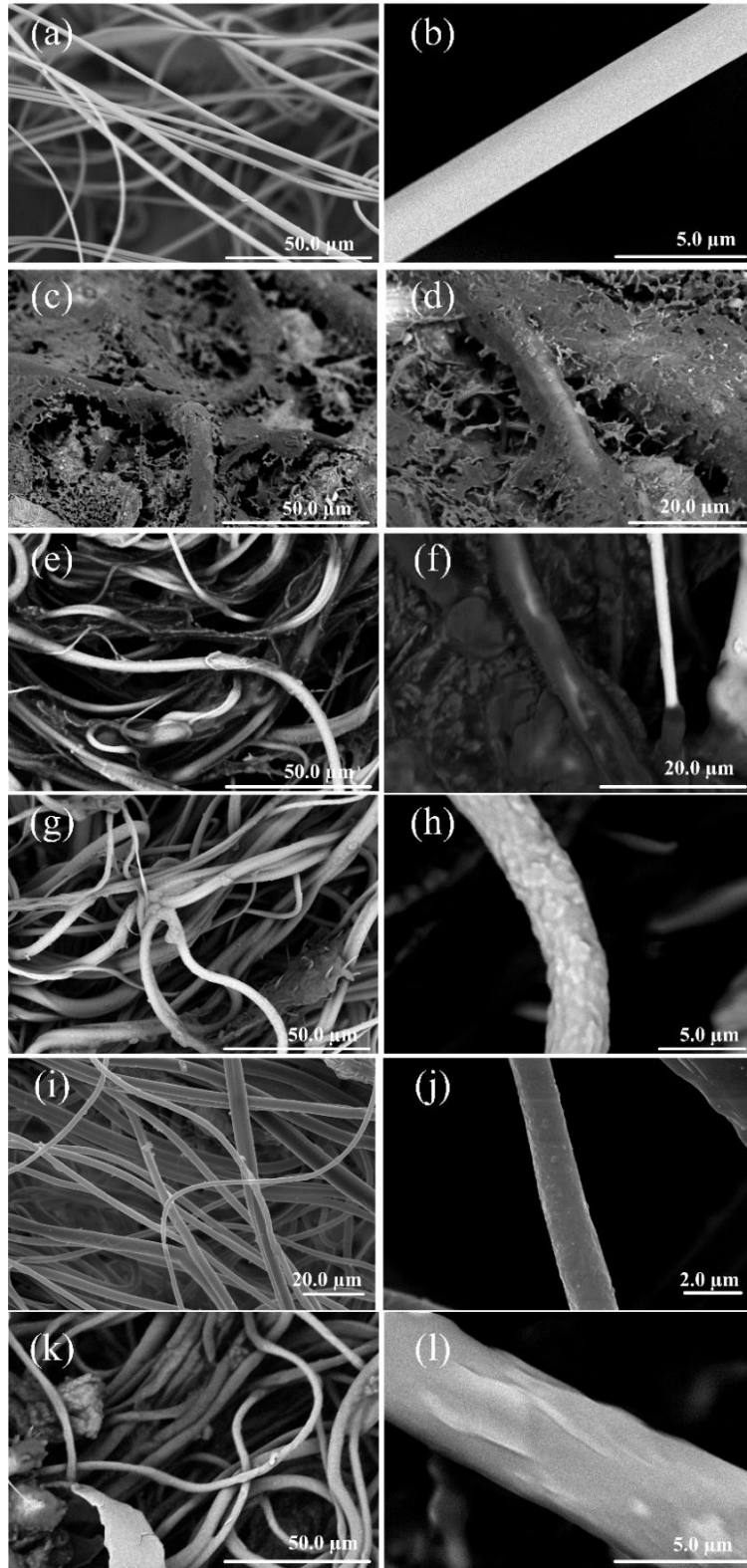
471 Based on Figure 5, the histogram shows the extraction yield using supercritical-CO₂ with total
472 of 41.17 wt. % over 8 runs at optimum condition of 80 °C and 200 bar. The first extraction resulted
473 in 22.00 % yield, about half of this amount (9.57 %) was further extracted from the same sample
474 PP-MNFs. The yield continued to drop by around half the previous amount until the 8th extraction,
475 the PP-MNFs weight remained constant indicating no residue oil is extracted at these conditions.

476 3.5. *Characterization of PP-MNF and oil extracted analysis*

477 3.5.1. *Physical and chemical properties of PP-MNF*

478 Polypropylene PP-MNF was fabricated using melt blowing system. The average diameter of
479 PP-MNF was ranging between 10² to 10⁴ nm, which indicates that this fiber consists of micro and
480 nanofiber. Figure 7 shows the SEM images of the PP-MNF, before, during and after oil recovery
481 experiment. The changes of physical structure were scanned with SEM analyzer and countable
482 images captured with vary magnifications (0.1 kX – 9.0 kX) and scales (500 μm – 5.0 μm),
483 depending on the availability and sharpness of the images obtained.

484



485

486 **Figure 7.** Morphology of the surface on the PP-MNF; (a, b) raw PP-MNF, (c, d) saturated PP-MNF, (e, f)
 487 pressed PP-MNF, (g, h) washed PP-MNF, (i, j) S-CO₂ PP-MNF and (k, l) reused PP-MNF

488 Figure 7a shows the raw PP-MNF that obtained at the collector was pile up and agglomerated
489 into bundles as a cotton-like. As discussed in section 3.2.1, the PP-MNF assembly has large pore
490 space, which contributes to large content of air gap. This could explained by the strand of PP-
491 MNF, which in disordered form, hence produced large pore and rough assembly surface. However,
492 the disordered PP-MNF could attributes more active sites for oil adsorption through intra pores
493 between fibrous [16], [55]. Thus, high oil adsorption capacity (Table 1) were obtained if exposed
494 to bulk of oil and high water uptake if exposed to water bulk (Figure 2). A strand of raw PP-MNF
495 image showed it has a smooth surface of morphology and clean fiber before adsorption, squeezing,
496 washing and extraction process (Figure 7b). This indicates that the fiber has a large surface area
497 for oil binding site [26].

498 The saturated PP-MNF that obtained during the adsorption process was expected wet and
499 occupies with oil adsorbed (Figure 7c), hence cold stage analysis were performed. Due to present
500 of oil, water and suspended solid in the POME [36], hence the oil adsorption were confirmed
501 containing water and oily sediments (Figure 2). The adhesion of suspended solid was due to the
502 intermolecular forces between layer of oil on the suspended solid and the PP-MNF [36]. Whilst,
503 water uptake was due to the interaction between water and air, hence leads the dispersed water that
504 trapped between the oil adsorption and the PP-MNF (Figure 3b). Figure 7d shows a strand of fiber
505 that covered with dark grey color, which assumed as frozen oil. Whilst, light grey color and anthill-
506 like assumed as frozen ice (water). Other than that, Zhou and co-workers [56] explained that the
507 adsorption water through hydrogen bonding exist between oil and water.

508 In physical desorption, manual pressing is a practical option and feasible for synthetic materials
509 [35], where highly strength to withstand the pressing force and durable. The PP-MNF used in this
510 work was synthetic, as it was made up by polypropylene based polymer. Hence, it was expected
511 to endure the pressure given to the PP-MNF for oil recovery. Figure 7e and 7d show the pressed

512 PP-MNF using hand pressing technique. No damage has been observed on the PP-MNF after one
513 time used and pressing. However, there were oil and oily sediments observed on the PP-MNF
514 (Figure 7e and Figure 7d). The adhesion of oil and sediments were due to London dispersion force
515 presents between solid non-polar molecule (the PP-MNF) and liquid non-polar molecule (the layer
516 of oil).

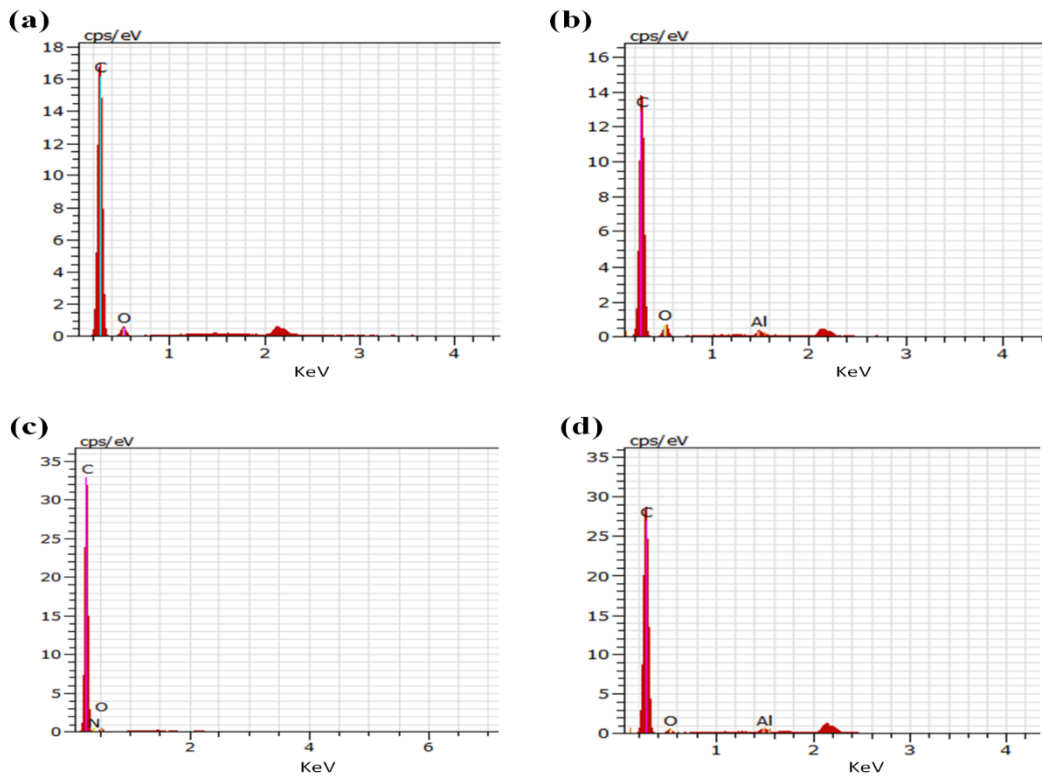
517 Figure 7g and Figure 7i show the washed PP-MNF and S-CO₂ PP-MNF, respectively. The PP-
518 MNFs were observed much clear, compared to the saturated and pressed PP-MNFs. These
519 indicating that the PP-MNFs have been regenerated by chemical extraction. However, changes on
520 PP-MNF morphology were observed (Figure 7h and Figure 7j), where the PP-MNF became shrink.
521 This could be suggested that the solvents (n-hexane and CO₂) have reaction with the PP-MNFs
522 surface. However, these changes has not been well understand, whether it is chemically changes
523 or only physically changes (i.e. porosity).

524 Lastly, the reused PP-MNF for 20 cycles were shown in Figure 7k and Figure 7l. No severe
525 damage have been observed, only several strand of PP-MNF were stretched (Figure 7l). This was
526 likely due to squeezing effect during desorption process. Thus, the mechanical and physical
527 desorption technique should be studied to optimize the oil recovery without damaging the fiber.
528 Somehow, solid particles were observed stuck between the fiber assemblies. This could explain
529 the increase of fouling effect, hence reduce the active sites for oil adsorption and the intermolecular
530 forces [16], [34].

531 The chemical composition of the polypropylene PP-MNF surfaces were analyzed by EDX
532 connected to the SEM. Figure 8 (a-d) showed the EDX spectra of raw PP-MNF, saturated PP-
533 MNF, pressed PP-MNF and washed PP-MNF samples, respectively. Table 3 shows the weight of
534 elemental composition in each PP-MNF. The signals of carbon (C) and oxygen (O) were observed
535 in every sample, where the weight of element C were increased as the PP-MNF used in oil

536 recovery. This could be due to present of residual oil on saturated and pressed PP-MNF. The
537 weight kept increasing on the washed PP-MNF was probably due to the presence of solvent
538 molecules which are mainly hydrocarbon group [32]. The EDX result on the washed PP-MNF
539 confirmed that the shrink PP-MNF (Figure 7h) was not chemically changes. Thus, it was suggested
540 by physically changes where the surface morphology was shrink due to cold solvents.

541 Whilst, the weight of O element showed inversely to C element, but slightly increased
542 compared to washed PP-MNF (Table 3). These results could supported by Fahma and co-workers
543 [57], where there is air exist in the PP-MNF and hydrogen bonding between residual oil-water.



544
545 **Figure 8.** EDX spectra of polypropylene PP-MNF; (a) raw fiber, (b) saturated fiber, (c) pressed fiber and
546 (d) washed fiber

547

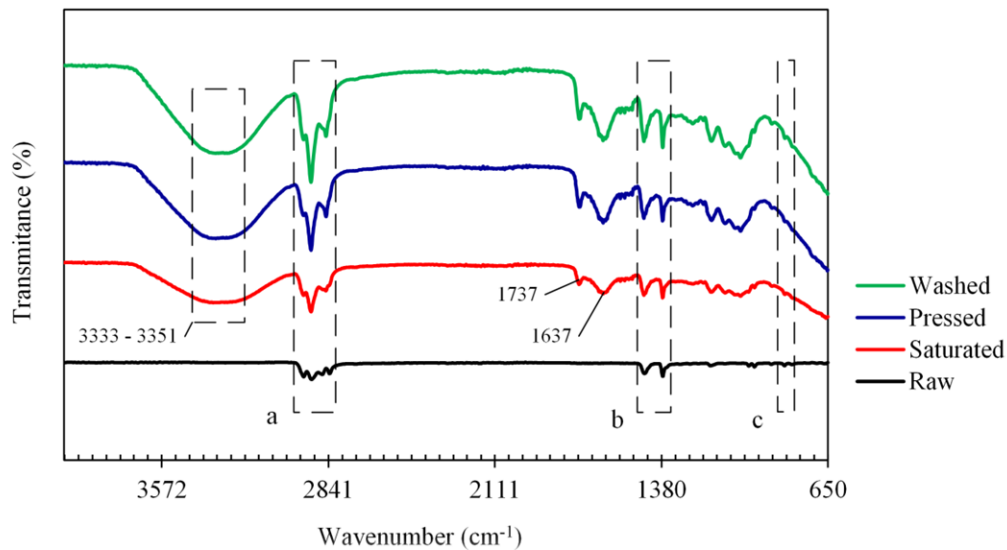
548

549 **Table 3.** Elemental compositions of PP-MNFs

PP-MNF	Weight of Carbon (C), %	Weight of Oxygen (O), %	Weight of Aluminum (Al), %	Weight of Nitrogen (N), %
Fresh	88.77	11.23	-	-
Saturated	88.93	9.10	1.97	-
Pressed	92.11	4.97	-	2.92
Washed	92.34	7.04	0.61	-

550

551 Other than that, the EDX spectra revealed the presence of aluminum (Al) and nitrogen (N) on
 552 the saturated, pressed and washed PP-MNFs, respectively. This is not surprised because the
 553 elements were contained in POME, such as phosphorus (P), potassium (K), magnesium (Mg),
 554 calcium (Ca), boron (b), iron (Fe), manganese (Mn), copper (Cu) and zinc (Zn) [6]. Hence, these
 555 elements could attributed from the suspended solid that stuck and adhered on the PP-MNF surface
 556 (Figure 7g).



557

558 **Figure 9.** FT-IR spectra of the polypropylene PP-MNF; (black line) raw PP-MNF, (red line) saturated PP-
 559 MNF, (blue line) pressed PP-MNF and (green line) washed PP-MNF

560 In addition to the SEM-EDX, changes on the chemical structure of PP-MNFs and to reveal the
 561 presence of oil component that was attached on the PP-MNF before, during and after oil recovery

562 were determined by FT-IR spectrometer. The FTIR spectra was recorded in the wavenumber range
563 of 600–4000 cm^{-1} . The FT-IR spectra of the raw PP-MNF exhibited peaks between 2950 cm^{-1} and
564 2860 cm^{-1} (Figure 9a inset). These peaks indicates the presence of symmetric stretching vibration
565 of $-\text{CH}_3$ group (2867 cm^{-1}) and asymmetric stretching vibration of $-\text{CH}_3$ and $-\text{CH}_2$ group (2949
566 cm^{-1} and 2914 cm^{-1} , respectively) [58] of the polypropylene structure. The structure was further
567 evidenced by the two peaks observed at 1452 cm^{-1} and 1373 cm^{-1} (Figure 9b inset), indicated the
568 presence of asymmetric and symmetric scissoring vibrations of the methyl group, respectively
569 [59]. Moreover, a weak peak at 840 cm^{-1} indicates of $-\text{CH}_2$ stretching [59].

570 Similar peaks were observed to the saturated PP-MNF, pressed PP-MNF and washed PP-MNF.
571 These indicated no chemical changes in polypropylene based PP-MNF. However, a strong band
572 between 3333 cm^{-1} to 3351 cm^{-1} were observed which attributed the presence of a broad
573 intermolecular hydrogen bonded (O-H) stretching [57]. The presence peaks between 1637 cm^{-1}
574 and 1737 cm^{-1} were observed respectively on the saturated, pressed and washed PP-MNF, where
575 the vibration of C=C stretching mode were attributed to the stretching of the carbonyl group [60].
576 A peak at 654 cm^{-1} were observed after adsorption, followed by desorption and it was represented
577 the presence of bending alkyne group. Therefore, these peaks revealed the presence of oil that
578 adsorbed on the polypropylene PP-MNF.

579 3.5.2. Components distribution as function of pressure and temperature

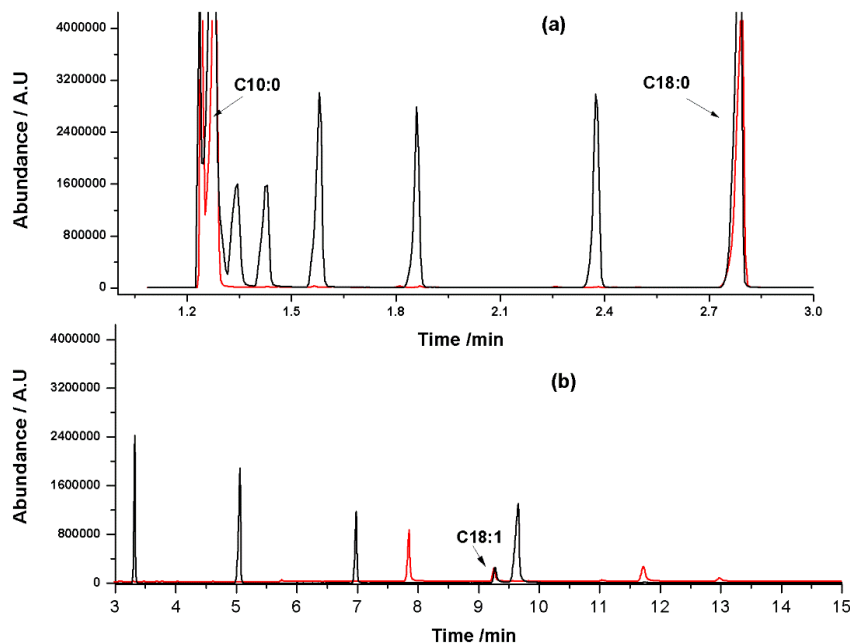
580 Table 4 shows fatty acids concentration in the extract as function of the pressure applied. Major
581 fatty acids detected are methyl decanoate C10:0, methyl stearate C18:0 and oleate C18:1. Saturated
582 fatty acids such as methyl decanoate C10:0 and methyl laurate C12:0 concentration increase with
583 high pressure this is explained by their highly solubility in sc- CO_2 . Whereas, unsaturated fatty acid

584 mainly methyl stearate C18:0 concentration decrease with high pressure. Methyl oleate C18:1
 585 concentration fluctuates with the pressure applied.

586 **Table 4.** Fatty acids concentration (ppm) in the extract by SFE CO₂ as function of the pressure applied

Pressure (bar)	C10:0	C18:0	C18:1	C12:0	C20:0
80	369.67	168.22	23.49	14.90	-
100	33.16	156.34	19.11	-	trace
120	21.58	153.87	30.06	156.10	-
150	35.71	119.21	17.31	156.42	-
200	29.09	158.67	26.12	-	-

587
 588 A chromatogram showing the oil extracted using sc-CO₂ (40 °C and 80 bar) and fatty acid
 589 methyl esters (FAME) standard mix is illustrated in Figure 10. The extracts at the conditions
 590 investigated were analyzed by UV-Vis from 250-600 nm wavelength. Carotene which absorbs
 591 light at 450 nm was not present in these extracts.



592
 593 **Figure 10.** Chromatograms of: (red) oil extract by SFE CO₂ at 40 °C and 80 bar and (black) FAME
 594 standards. (a) Retention time 1 to 3 min. (b) retention time 3 to 15 min.

595 **4. Conclusions**

596 The potential of PP-MNF as oil adsorbent in POME had been investigated. The oil adsorption
597 capacity of PP-MNF using refined palm oil was 28.65 g of oil/ g of PP-MNF in average, whilst
598 the oil recovery from POME was 10.93 g of oil/g of PP-MNF. The yield of physical extraction
599 using hand pressing was 89.62% in average, where the rest still retained in the PP-MNF. The
600 chemical extraction was performed and the yield were comparable between the solvent and
601 supercritical CO₂ extraction techniques which 62.44% and 41.17%, respectively and these
602 techniques contributed to the regeneration of used PP-MNF. No significant physical changes were
603 observed on the PP-MNF using FTIR and EDX, however extraction using solvents showed
604 significant change was detected to the PP-MNF using SEM. No trace of polypropylene was
605 detected using GC-MS in the recovered oil, suggesting that the PP-MNF did not dissolved into the
606 oil during the recovery process. The PP-MNF showed significant reusability after 20 trials
607 indicating high commercial value. The limitation of the study lies in the representation of POME
608 samples. In an actual situation, the concentration of oil in POME varies over time, this is contrary
609 to the POME sample used in this study. Hence, future work can be done by performing the study
610 on mill site to get realistic POME samples. In addition, the pressing of PP-PP-MNF can also be
611 mechanized in order to get consistent and replicable force. All in all, this study shows that PP-MF
612 is commercially viable to recover residual oil from POME.

613 **Acknowledgement**

614 **References**